Spectral editing: A quantitative application of spin-echo nuclear magnetic resonance spectroscopy to the study of ^{27}Al in zeolite catalysts

Kirk D. Schmitt
Central Research Laboratory, Mobil Research and Development Corporation, Princeton, NJ, USA

Jürgen Haase and Eric Oldfield
Department of Chemistry, University of Illinois at Urbana-Champaign, Urbana, IL, USA

^{27}Al spin-echo nuclear magnetic resonance (n.m.r.) is used to measure the spin–spin relaxation times, T_{2H}, for a substantial number of model compounds, and a theory (with no adjustable parameters) based on Al–Al dipolar interactions combined with crystallographically determined Al–Al distances is used to estimate T_{2H}. The homonuclear magnetic dipole interaction explains the experimental data reasonably well for compounds with high Al levels, but much less well for compounds with low levels of Al, where structure-specific interactions are important. Such structure-specific interactions are exploited to edit zeolitic Al from the background binder in alumina-bound ZSM-5 and in dealuminated zeolite-Y catalysts containing nonframework (NFW) Al. Editing allows quantitative analysis of the zeolitic components. For dealuminated zeolite Y, it is concluded that peaks assigned by others to "pentacoordinate" Al may actually arise from NFW aluminum, based on the fact that their T_{2H} is short relative to framework (FW) Al. Theory and experimental results for the technically more demanding measurement of T_{2H} under conditions of "magic-angle" sample spinning (*MAS*) with synchronous sampling are also reported. Spin-echo editing of synchronously sampled ^{27}Al *MAS* n.m.r. spectra are shown to be useful for determining the FW zeolitic Al content of realistically formulated (kaolinite bound) and steamed/calcined fluidized bed cracking (FCC) catalysts. The loss of framework Al in two series of steamed FCC catalysts is less precipitous than the loss in catalytic activity, as measured by the hexane cracking α parameter.

Keywords: Spin-echo editing; alumina bound catalysts; aluminum n.m.r.; steam cracking; kaolinite theory

INTRODUCTION

"Magic-angle" sample spinning (*MAS*) ^{27}Al nuclear magnetic resonance (n.m.r.) spectroscopy of zeolites has been much used in the last decade. Application to the commercially important zeolites ZSM-5[1–35] and zeolite Y[1,10,11,18,20,23,25,36–65] has been particularly intense, but has never shown the kind of high resolution achieved for silicon or carbon. For example, ^{29}Si n.m.r. spectra of the framework silicons of ZSM-5 may show all 12 or 24 lines expected in the orthorhombic or monoclinic forms,[66] but ^{27}Al n.m.r. never shows more than two lines.[9] This lack of resolution arises primarily because of quadrupolar broadening, and an unresolved chemical shift distribution among the numerous (12 or 24) tetrahedral Al sites. Lack of resolution is even more serious for mixtures of aluminum species, such as occur in alumina,[58] silica/alumina,[60] or clay bound[61,62] zeolites, or in unbound zeolites where nonzeolitic aluminum has been produced by thermal[4,18,23,37,38,56,59] or steam treatments.[28,32,51,53]

Lack of true high resolution has necessitated the use of other parameters in addition to the familiar chemical shift to characterize zeolites.[67] Among these are the line width; the nuclear quadrupole coupling constant; and the asymmetry parameter. Line-width measurements are not particularly useful for mixtures since the zeolite is often buried under a broad background signal from Al-containing binders. For relatively simple systems, like ZSM-5 bound with γ-alumina, or pure zeolite Y that has been steamed or calcined, several techniques are, however, available for determining framework aluminum content. For example, the matrix or nonframework aluminum

Address reprint requests to Dr. Schmitt at the Central Research Laboratory, Mobil Research and Development Corporation, P.O. Box 1025, Princeton, NJ 08540, USA.
Received 13 January 1993; revised 21 June 1993; accepted 8 July 1993

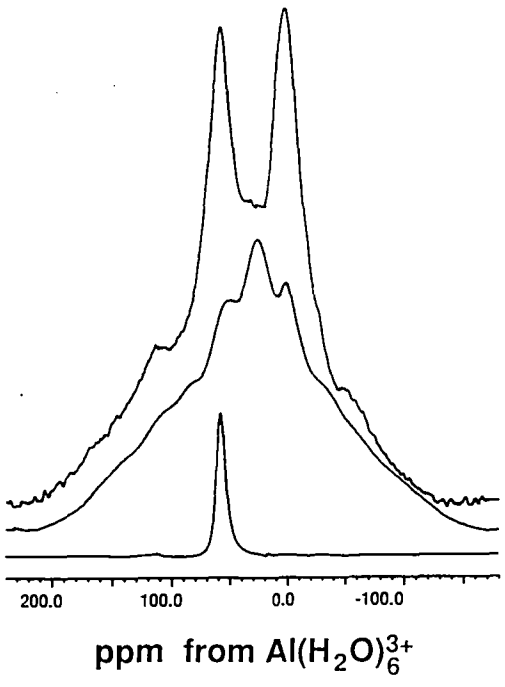

Figure 1 8.45 Tesla ^{27}Al *MAS* n.m.r. spectra of a 10 h steamed commercial FCC catalyst (top), a 500°C calcined kaolinite (middle), and an as-synthesized zeolite Y (bottom).

may be removed chemically with acetylacetone[68] or HCl,[45] or differential quadrupole couplings can be exploited to obtain enhanced resolution in 2-dimensional n.m.r. by taking advantage of the differential pulse responses of materials with large and small quadrupole coupling constants.[10,14,22,23,49,50,59] Selection for materials with small coupling constants can be achieved using suitably long pulses[22] or by operating at low magnetic field strengths, where large coupling constant materials suffer from extreme broadening and quadrupole-induced shifts. Recently introduced double-angle spinning[69,70] techniques may also be helpful, in principle. Moreover, it has recently been claimed that editing may be based on the differential T_1 between zeolite Y and γ-alumina,[58] but this is expected to give only very weak selectivity.[65]

Figure 1 illustrates the type of problems encountered when carrying out ^{27}Al n.m.r. studies on a typical commercial clay-bound zeolite Y. It compares a 360 MHz ^{27}Al n.m.r. spectrum of a 10 h steamed commercial catalyst (top) with a 500°C calcined kaolinite (middle) and an as-synthesized zeolite Y and demonstrates the typical problems observed, i.e., grossly overlapping peaks from four, five, and six coordinate aluminum from the zeolite and four, five, and six coordinate aluminum resonances from the clay. It has been claimed that "fast *MAS*" and very high fields[60] will eliminate these problems for steamed zeolite Y, but no such claims are made for clay[62] or alumina-bound materials, where spinning or field cannot separate peaks that intrinsically overlap. The assignment of a peak at ~ 30 ppm to pentacoordinate Al is also controversial.[23,42,45,46,50,51,53,59–61]

Thus, improved methods are required in order to "edit" away nonzeolitic peaks, enabling a quantitative analysis of the framework zeolites in commercial catalysts, and in this paper, we report on recent progress using the spin–spin relaxation time, T_{2H}, determined from a "Hahn" echo, as an editing parameter.

As long ago as 1959, Spokas and Slichter showed that T_{2H} can be determined in aluminum metal[71] using a (in-phase) Hahn echo. The apparatus was quite simple and easily adapted to variable temperature experiments up to the melting point of aluminum. Echo measurements of T_{2H} for ^{27}Al have since been reported for $Nb_3Al_{1-x}Ge_x$ alloys[72] (^{93}Nb as well) and aluminum–plutonium–uranium alloys,[73] and T_{2H} results for ^{23}Na (but not ^{27}Al) have been reported for β-alumina.[74] In 1978, Resing and Rubinstein[75] applied ^{27}Al spin echo n.m.r. to characterize Linde 13X before and after dehydroxylation and also measured the T_{2H} of an (unspecified) alumina.

The spin echo experiment uses a very simple 90-τ–180-τ pulse sequence, and the theory as applied to quadrupolar nuclei has been discussed elsewhere.[76] If low-power pulses are used for ^{27}Al nuclei, so that the central transition is excited selectively, such "soft pulse" excitation has been shown to give a quantitative spin echo response.[77] The intensity of the echo that forms at the end of the second evolution period can be approximated for short times as an exponential function of τ, Equation (1):

$$E(2\tau) = E_0 e^{-\left(\frac{2\tau}{T_{2H}}\right)^2} \quad (1)$$

Haase and Oldfield[76,77] showed that homonuclear dipolar interactions, strong heteronuclear dipolar interactions, and chemical shift differences will all affect T_{2H}. If only a homonuclear dipolar coupling (I-spins, only) is present, the corresponding nuclei experience the same quadrupole coupling, and their chemical shift difference is small compared with the dipole interaction, then the spin-echo decay is given by[76]

$$T_{2H} \approx 1.5\sqrt{\frac{2}{M_{2F}}} \equiv 1.5\,T_{2F} \quad (2)$$

where M_{2F} is the ordinary Van Vleck second moment of the homonuclear dipolar interaction and T_{2F} is the $1/e$ time constant of a Gaussian free-induction decay.

As the difference in the chemical shift of two neighboring spins increases, and eventually exceeds the homonuclear dipolar interaction, the spin-echo decay slows because of suppressed spin-flipping. The corresponding maximum T_{2H} is then given by[76]

$$T_{2H} = \sqrt{k(I)}\;T_{2F} \quad (3)$$

where $k(I)$ = 4/81, 4/321, 4/881, and 4/1961 for I = 3/2, 5/2, 7/2, and 9/2, respectively.

Additional heteronuclear dipolar interaction (I–S

interaction) has a similar effect in depressing the spin-flipping among like transitions and thus increases T_{2H}. However, spin-flipping in the S-spin system eventually limits the increase in T_{2H} of the I-spins, and as a good approximation one can write[76]

$$T_{2H} = \sqrt{\frac{2}{k(I) \cdot M_{2F}(I) + k(S) \cdot M_{2F}(S)}} \quad (4)$$

where $M_{2F}(I)$ and $M_{2F}(S)$ represent the Van Vleck second moment for homonuclear dipolar interaction in an unperturbed I- and S-spin system, respectively. If the S-spin system is not subjected to a strong quadrupolar coupling (compared with its homonuclear dipolar interaction) or represents a spin-1/2 system, $k(S) = 1$. Special cases, e.g., for weak I–S coupling, can only be estimated from Equations (3) and (4). For most zeolites at room temperature, the interactions of the quadrupolar nuclei with the ^1H nuclei are typically averaged, as is the dipolar interaction with cations in hydrated samples.

The homonuclear Van Vleck second moment can be written as

$$M_{2F} = \gamma^4 \hbar^2 \frac{3I(I+1)}{5} \sum_j \frac{1}{r_{ij}^6} \quad (5)$$

The methods developed for "T_{2H} editing," as well as characteristic T_{2H} values for a number of model compounds—aluminas, silica/aluminas, and kaolinite/metakaolinite—are the subjects of this paper. T_{2H} editing will be applied to both ZSM-5 and zeolite Y catalysts, bound and unbound, and in various states of calcination and steaming, and we show by judicious variation of pulse separation, τ, in low-power spin-echo experiments, that a relatively clean and quantitative separation of zeolitic v. binder signals can be achieved.

EXPERIMENTAL

Chemical aspects

Samples were run either as received ("atmospheric humidity"), after overnight equilibration in a dessicator at 52% relative humidity (over a saturated solution of $NaHSO_4$) or after adding sufficient liquid water so that excess water could be seen in the sample tube.

Some materials were obtained from commercial sources: α-alumina monohydrate (Kaiser); corundum (Fisher Scientific); G-958 silica/alumina (Davison); and amorphous $AlPO_4$ (Alfa). Others were obtained as gifts: berlinite $AlPO_4$ (Mark Davis of Virginia Polytechnic Institute and State University) and as-synthesized $AlPO_4$-17 (H. W. Solberg of Mobil). Others were prepared as described in the literature: as-synthesized $AlPO_4$–5 (Ref. 78); as-synthesized SAPO-11 (Ref. 78); as-synthesized SAPO-37 (Ref. 78); as-synthesized Na zeolite Y (Ref.79); Breck structure six faujasite (Ref. 80); zeolite beta (Ref. 81); ZSM-5 (Ref. 82); and a boron-containing ZSM-5 (Ref. 83). A second sample of corundum was prepared by calcining Catapal-S for 15 h at 1200°C, in flowing air.

Amorphous silica/aluminas were made as follows: To 4.95 g HiSil (Degussa) and 0.54 g PHF alumina (Cyanamid) in 14.5 ml H_2O were added 5 ml 7.4 M NH_4OH, gradually, with stirring. The slurry was dried in a 5–8 cm deep bed at 150°C, then calcined under flowing air by programmed heating at 2°C/min. to 540°C. After 4 h at 540°C, the product was cooled under flowing N_2. This product is designated 0.5% Al HiSil/PHF silica/alumina. The 1% and 2% products were made the same way with 2× and 4× the quantity of PHF alumina. To 5.0 g Cabosil-M5 (Cabot) and 0.268 g PHF alumina (Cyanamid) in 13 ml H_2O were added 5 ml 7.4 M NH_4OH, gradually, with stirring. The slurry was dried in a 5–8 cm deep bed at 150°C, then calcined under flowing air by programmed heating at 2°C/min to 540°C. After 4 h at 540°C, the product was cooled under flowing N_2. This product is designated 0.25% Al Cabosil/PHF silica/alumina. The 0.134% and 0.067% products were made basically the same way but with 0.5× and 0.25× the quantity of PHF alumina. XRD confirmed the silica/aluminas to be amorphous; elemental analysis (Galbraith) confirmed the aluminum concentrations.

The NH_4^+ exchanged silica/alumina was prepared from G-958 silica/alumina. After drying 5 g of G-958 under flowing N_2 at 300°C for 2 h, it was cooled, saturated with flowing NH_3 at 100°C, cooled to room temperature, stirred 2 h with 200 ml 1.0 N NH_4Cl, filtered, washed with 100 ml H_2O, then dried. No NH_3 could be removed from this sample by boiling with H_2O.

The anhydrous, propylamine-containing ZSM-5 was obtained by heating a 1 g Si/Al_2 70:1 NH_4-ZSM-5 sample at 2°C/min to 120°C, holding 1 h at 120°C, ramping 5°C/min to 500°C, then holding 10 h at 500°C, followed by cooling quickly to room temperature, all at 0.05 Torr. The sample was packed into a rotor in a dry glove box, then 35 μl amine were added using a 100 μl syringe (7 drops), and the rotor sealed before removing from the glove box. The amine had been dried overnight over 4Å sieves.

All the zeolite Y samples, with the exception of the as-synthesized Y, were commercially available from TOSOH. The properties of the TOSOH samples are described in literature from that company. USY FCC catalyst from Davison (< 0.2% rare earth, "RE") was steamed 10 h at 790°C under 45% steam. The USY FCC catalyst consists of approximately 30% USY in a matrix containing silica–alumina. Fresh, steamed, and calcined REUSY catalysts from Davison (*Table 1*) were obtained from G. W. Woolery of Mobil's Paulsboro Laboratory. The REUSY catalyst is 35% USY with ~ 2.6% rare earth in a silica–alumina matrix, presumed to be kaolinite derived. Except for the "fresh" catalyst, which was in the NH_4^+ form, all the catalysts were H^+ forms.

The kaolinite was API Clay Mineral Standards Project kaolinite #9 from Mesa Alta, New Mexico. A series of samples in progressive states of dehydration and conversion to metakaolinite was prepared by

Table 1 Treatment conditions for commercial FCC catalysts

Sample	Treatment
USY catalyst	None
Steamed USY catalyst	10 h 790°C, 45% steam
Fresh REUSY catalyst	None
Calcined REUSY catalyst	Calcined 2 h 650°C
5 h REUSY catalyst	5 h 760°C, 100% steam
10 h REUSY catalyst	10 h 760°C, 100% steam
20 h REUSY catalyst	20 h 760°C, 100% steam

heating ~ 3 mm deep beds in a Pt crucible in air at 300, 400, 500, 700, 800, 900, and 1000°C for 3 h after a 20°C/min heat-up. The conversion was confirmed to have progressed as described in the literature[84] by comparing ^{27}Al *MAS* n.m.r. spectra with those in the literature and by obtaining X-ray diffraction patterns, which clearly showed loss of crystallinity in samples calcined above 400°C.

Catalytic activity

Hexane cracking rates relative to an amorphous silica/alumina, "α," were measured as described elsewhere.[21]

N.m.r. spectroscopy

^{27}Al n.m.r. spectra were run on a Chemagnetics 360 MHz (^{1}H resonance frequency) CMX n.m.r. at Mobil and on a home-built 500 MHz (^{1}H) n.m.r. at the University of Illinois. Standard *MAS* probes were used with aluminum-free zirconia rotors at Mobil and nonspinning single resonance probes with quartz or Teflon tubes at the University of Illinois. The spin-echo technique is capable of detecting impurity levels of Al in zirconia not normally seen under *MAS*. These impurities have broad lines and long T_{2H}'s (presumably reflecting a dilute state). Rotors were selected based on the criterion that they showed no spin-echo signal after 500,000 scans at a 250 μs τ-delay.

The pulse sequence used was 90x-τ-180x-τ-acquire, with phase cycling of 0, 90, 270, 180, 180, 270, 90, 0 for pulses and acquisition. High-power proton decoupling was used where appropriate. The experiments were typically set up on a Si/Al_2 70:1 ZSM-5, or a 5 μl solution of $AlCl_3$. Power levels were adjusted to obtain a solution 90° pulse of 40–60 μs. Voltage missetting corresponding to ~ 15% on the 90° pulse length resulted in measured T_{2H} values being ~ 5% too long, and E_0 intercepts ~ 15% too small, for the 70:1 ZSM-5 sample. Smaller missettings resulted in correspondingly smaller errors.

Generally, the number of scans was incremented upward by a factor of 1.25 as τ incremented upward by 100–400 μs (enough to decrease the signal by ~ 20%). In this way, most of the acquisition time was devoted to those spectra in which the signal to noise (*S/N*) ratio was low and not wasted on the high *S/N*, short-τ data sets. This shortened data acquisition times by factors of ~ 10–90 with no sacrifice in data reliability v. an experiment in which the number of scans was kept constant for all τ values. Signal intensities were normalized for number of scans and sample weight before quantitative calculations were made. Experiments took from 5 min to overnight to complete, depending on concentration, the number of τ values, and the spectrometer used.

For quantitative measurements, we found it most practical and reliable to either determine the 1/*e* decay time constant, T_{2H}, or to fit the overall spin-echo decay to a single or double exponential. For a single exponential, a linear regression on the log of intensity vs. time was used. For a double exponential, a nonlinear least-squares (Levenberg–Marquardt) procedure was used to minimize errors on the log of the residual intensity calculated from the double exponential decay. Although the shape of the spin-echo decay has been found to be Gaussian for very short τ values and dense spin-systems, for more dilute spin-systems and for longer τ values, the shape of the spin-echo decay is mostly exponential.[76] In either case, the 1/*e* time constant, T_{2H}, for the spin-echo decay is in good agreement with the theoretical time constant, calculated from the second moment of the spin-echo decay, assuming Gaussian behavior. Furthermore, excitation effects have been shown to influence the shape of the spin-echo decay for $\tau < T_{2F}$, the time constant of the free induction decay.[77]

To minimize the effects of nonselective excitation,[77] nearly all spectra were obtained on resonance with weak or soft pulses and with 2τ values up to at least 7–10 ms (for $T_{2H} > 1$ ms) or 3–4 ms (for $T_{2H} < 1$ ms).

MAS experiments were performed using the Chemagnetics automatic rotor-speed-controller, which regulates spinning speed to ±1 Hz at 2.5 kHz, and ±2 Hz at 6 kHz. This results in an error of no more than ~ 0.15° in rotor position, under synchronous sampling conditions. *MAS* spectra obtained on fully hydrated samples were obtained with 70–110% as much water as solid sample. The standard Chemagnetics zirconia rotors retained ≥ 90% of this water, even after spinning overnight at 5.5 kHz.

RESULTS AND DISCUSSION

A wide range of Al-containing materials was studied under quite varying conditions of sample humidity, in order to establish an experimental database. *Table 2* collects the T_{2H} data for all samples studied under static (nonspinning) conditions.

Table 2 lists T_{2H}s and Al concentrations, and it is clear that Al concentrations can be only roughly related to the sum of the internuclear Al–Al distances. For this reason, a systematic analysis of as many structures as possible was carried out in order to determine these sums more quantitatively. The program ORTEP[85] allows direct calculation of all interatomic distances within a given radius from a specified atom. Radii of 9–12 Å, which included from 100 to 200 Al–Al interactions, gave convergence in Σr_{ij}^{-6} calculations to within 1%. Al–Al distances were calculated without assumptions for compounds with 100% site occupancy of Al using crystal structure

Table 2 Compilation of ^{27}Al spin-echo n.m.r. results on various static samples

Sample	% Al[a]	f[b]	T_{2H} (ms)	N.m.r.[c]	Hydration[d]
Al (Ref. 71)	100.0	1.00	0.048	42	0
AlN (sample 1) (Ref. 76)	65.9	1.00	0.18	500	0
AlN (sample 2) (Ref. 76)	65.9	1.00	0.21	500	0
AlN (sample 3) (Ref. 76)	65.9	1.00	0.26	500	0
Al_2O_3 ruby single crystal (Ref. 76)	52.9	1.00	0.13	500	0
Al_2O_3 sapphire single crystal (Ref. 76)	52.9	1.00	0.13	500	0
Al_2O_3 corundum (Fisher Scientific)	52.3	1.00	0.13	360	0
Al_2O_3 corundum (Ref. 76)	52.9	1.00	0.14	500	1
Al_2O_3 corundum	52.9	1.00	0.20	360	0
Al_2O_3 ? (Ref. 75)	52.9	1.00	0.35	88	2
Al_2O_3 γ-alumina	52.9	1.00	0.30	500	1
AlOOH α-alumina Monohydrate KSAM	45.0	1.00	0.14	360	1
$AlPO_4$ amorphous (Alfa)	22.1	1.00	1.023	360	1
$AlPO_4$ Berlinite (M.E. Davis)	22.1	1.00	1.234	360	1
$AlPO_4$-5 as-syn.	22.1	1.00	0.634	360	1
$AlPO_4$-17 as-syn.	22.1	1.00	0.326	360	1
SAPO-11 as-syn.	20.0	1.00	0.561	360	1
SAPO-37 as-syn.	22.4	1.00	0.524	360	1
Linde A (Ref. 76)	19.2	0.85	0.730	500	3
Linde-13X (Ref. 75)	13.6	0.92	0.592	88	2
Linde-13X large xtal as-syn. (Ref. 75)	13.6	0.92	0.462	88	2
Linde-13X "dealuminated" (Ref. 75)	<13.6	0.56	0.491	88	2
Na zeolite Y as-syn.	9.2	0.16	0.777	360	1
Na zeolite Y as-syn.	9.2	0.16	0.80	500	1
Na zeolite Y as-syn.	9.2	0.16	0.94	360	3
Faujasite Breck structure six	9.2	0.16?	0.623	360	1
Zeolite beta	2.1	0.12	0.627	360	1
Silica/alumina H form G-958	6.4		1.33	360	2
Silica/alumina NH_4-exchanged G-958	6.4		1.25	360	2
Silica/alumina NH_4-exchanged G-958	6.4		0.98	500	1
Silica/alumina HiSil/PHF	2.0		0.93	360	2
Silica/alumina HiSil/PHF	2.0		1.00	500	3
Silica/alumina HiSil/PHF	1.0		1.18	360	2
Silica/alumina HiSil/PHF	1.0		1.20	500	3
Silica/alumina HiSi/PHF	0.5		1.84	360	2
Silica/alumina HiSil/PHF	0.5		1.60	500	3
Silica/alumina Cabosil/PHF	0.25		1.20	500	3
Silica/alumina Cabosil/PHF	0.125		1.40	500	3
Silica/alumina Cabosil/PHF	0.067		1.10	500	3
ZSM-5 NH_4	1.99	0.11	4.50	500	3
ZSM-5 $PrNH_2$	1.28	0.0072	0.64	360	0
ZSM-5 NH_4	1.28	0.0072	3.00	360	1
ZSM-5 NH_4	1.28	0.0072	5.03	360	3
ZSM-5 H	1.28	0.0072	5.61	360	3
ZSM-5 NH_4	1.21	0.0068	2.17	360	1
ZSM-5 NH_4	1.13	0.0064	3.70	500	3
B-ZSM-5	1.00	0.0056	1.60	360	1
B-ZSM-5	1.00	0.0056	2.52	360	2
B-ZSM-5	1.00	0.0056	3.70	360	3
ZSM-5-NH_4	0.64	0.0036	3.24	360	1
ZSM-5 NH_4	0.61	0.0034	3.35	500	3
ZSM-5 NH_4	0.135	7.51e-4	4.70	500	3
ZSM-5 NH_4	0.066	3.66e-4	3.35	360	1
ZSM-5 NH_4	0.066	3.66e-4	2.80	500	3

[a] Not ash corrected, may be approximate or calculated from ideal formula
[b] Fraction of available sites filled by Al (assumes Al–P alternation and Loewenstein's rule)
[c] Proton n.m.r. resonance frequency of spectrometer used to obtain ^{27}Al data
[d] 0 = dry; 1 = atmospheric humidity; 2 = 52% relative humidity; 3 = H_2O saturated

data and occupancy factors in which the sites were reported to be ordered. For zeolites with less than 100% occupancy, or where no ordered structure has been reported, Lowenstein's rule was assumed for next nearest T-atom neighbors and a random siting of atoms in all other locations. SAPOs were assumed to be $AlPO_4$'s with strict alternation of Al–O–T. This is certainly true for SAPO-37 (Ref. 86) and probably true for SAPO-11, since its Si concentration was quite low. *Table 3* summarizes the results. It is interesting that for some structures, such as zeolite beta, there is almost a factor of two (1.8) spread in Al–Al inter-

Table 3 Al–Al interactions of various crystallographic sites[a]

Sample	Site	Σr_{ij}^{-6} 10^{-6} pm^{-6}	Structure reference
Al metal	1	25900	87
Al_2O_3 corundum	1	17600	88
AlN aluminum mononitride	1	16400	89
Berlinite ($AlPO_4$)	1	2520	90
FAU ordered structure	1	659	91
FAU disordered structure	1	811	91
LTA	1	621	92
Breck structure 6 faujasite	1	878	93
	2	874	93
	3	874	93
	4	870	93
AFI ($AlPO_4$-5)	1	840	94
$AlPO_4$-17	1	962	95
	2	695	95
SAPO-11 ordered	1	638	96
	2	792	96
	3	937	96
Beta	1	1041	97
	2	1046	97
	3	980	97
	4	993	97
	5	1538	97
	6	1509	97
	7	900	97
	8	857	97
	9	933	97
ZSM-5	1	993	98
	2	1224	98
	3	1400	98
	4	1191	98
	5	1114	98
	6	1015	98
	7	1064	98
	8	1064	98
	9	1364	98
	10	1118	98
	11	1083	98
	12	1038	98

[a] Site numbering schemes are those given in the literature references

action for different crystallographic sites. However, the $1/\sqrt{\Sigma r_{ij}^{-6}}$ will reduce this to a range of ±17% in T_{2H}.

Now, if homonuclear Al–Al dipolar interactions alone determined T_{2H}, a plot of T_{2H} vs. $1/\sqrt{\Sigma r_{ij}^{-6}}$ would be a straight line. *Figure 2* shows such a plot, along with the theoretical relationship calculated from Equations (2) and (5). Only materials with occupancy factors $f > 0.9$ are included on this plot, since all materials with $f < 0.9$ have T_{2H}s well below the theoretical line. For materials with multiple sites, separate points have been added for each ORTEP derived Σr_{ij}^{-6}, even though a single T_{2H} was obtained experimentally. There is quite good agreement between the experimental T_{2H} and the theoretical expectation for a purely homonuclear dipole interaction (in the approximation of a Gaussian T_{2H}), particularly since there are no adjustable parameters. We found only one exception, the berlinite sample: T_{2H} = 1.23 ms, compared with an expected value of about 0.35 ms. The result for berlinite shows that there has to be a suppression of spin exchange, such as a chemical-shift nonequivalence, or a very different quadrupole coupling for neighboring Al nuclei. Haase and Oldfield[76] calculated up to a sixfold increase in T_{2H} if spin exchange is completely suppressed. This probably explains the deviation of berlinite, since this material contains numerous imperfections in the form of H_2O inclusions,[99] which result in supersaturated point defect concentrations on annealing.

Zeolites with occupancy factors < 0.9 show T_{2H} values too small to be accounted for by homonuclear dipolar interactions alone. One factor that may be important is the heteronuclear ^1H–^{27}Al dipolar interaction. This interaction should decrease for very wet zeolite samples, where dipolar interactions will be motionally averaged, and this is borne out by the hydration results shown in *Table 2*. For a fully hydrated (wet) sample, the same sample showed a T_{2H} of 5.6 and 5.0 ms—for the H^+ and NH_4^+ forms, but equilibrated at 52% humidity, it exhibited a T_{2H} of 3.0 ms. A very dry sample containing a small amount of $PrNH_2$ showed a relatively sharp signal, with T_{2H} = 640 μs. These results clearly show that H_2O or other polar molecules may influence the T_{2H} of zeolites. However, H_2O has only an extremely small effect on the T_{2H} of silica–aluminas, which are all short,[67] which enables us to use T_{2H} as an editing tool in complex zeolite catalysts, as discussed in detail below. Also, we note here that T_1 effects make only a minor contribution in most of the cases that we have examined.

The T_{2H} of materials with occupancies below < 0.9 is consistently less than expected from homonuclear dipole interactions and varies among different samples. ZSM-5 materials, all of which have occupancies < 0.02, seem to show no relationship between T_{2H} and Σr_{ij}^{-6}. Results on Y zeolites, obtained with identical counterions, identical hydration states, and occupancies from 0.16 to 0.00133, do, however, show a linear relationship between T_{2H} and $1/\sqrt{\Sigma r_{ij}^{-6}}$,

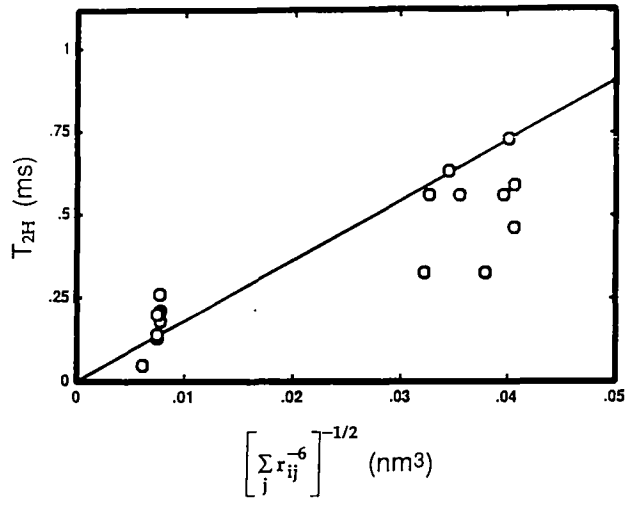

Figure 2 Plot of T_{2H} vs. $1/\sqrt{\Sigma r_{ij}^{-6}}$ for Al-containing materials. The straight line is the theoretical line calculated with no adjustable parameters, from Equations (2) and (5) in the text.

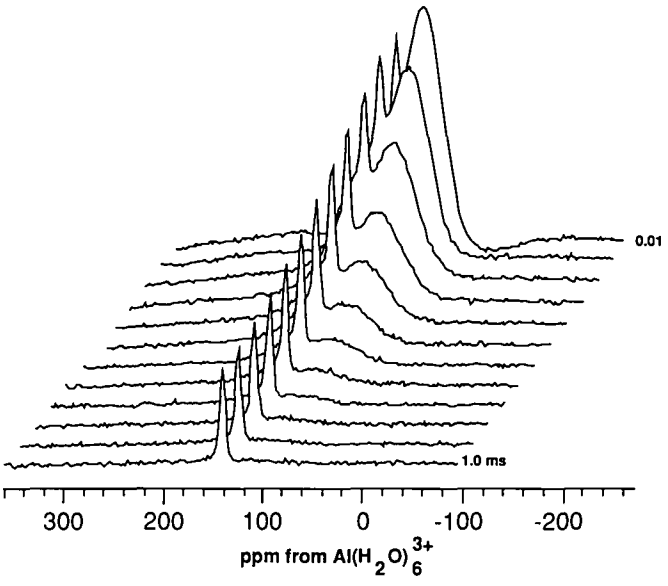

Figure 3 11.7 Tesla ^{27}Al n.m.r. spin-echo spectral editing of Al in a 63:37 mixture of a 140:1 Si/Al$_2$ ZSM-5 and γ-alumina. The τ's from top to bottom were 0.01, 0.05, 0.1, 0.2, 0.3, 0.4, 0.5, 0.6, 0.7, 0.8, 0.9, and 1.0 ms. The ratio of alumina Al to zeolite Al was 40:1.

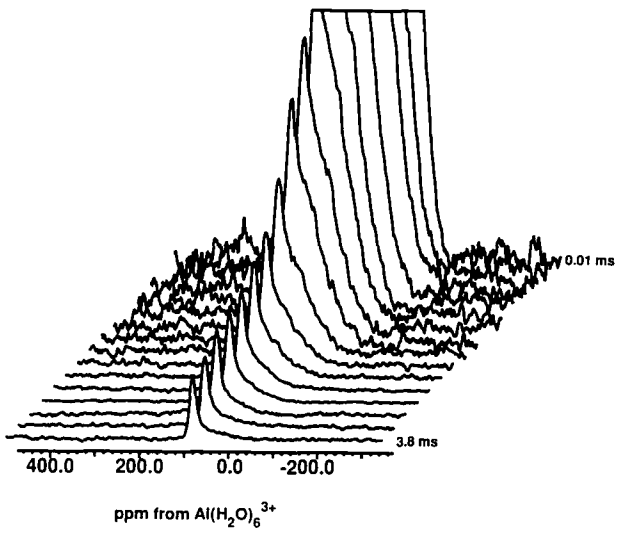

Figure 4 8.45 Tesla spin-echo spectral editing of Al in a commercial, dealuminated zeolite Y, TOSOH HSZ-360HUA. The τ's from top to bottom were 0.1, 0.3, 0.5, 0.6, 0.7, 0.8, 1.0, 1.2, 1.4, 1.6, 1.8, 2, 2.4, 2.8, 3.2, and 3.8 ms.

although the slope of the line is not the theoretical one based on homonuclear dipole coupling. The series of silica/aluminas shown in *Table 2* is also particularly striking: Despite wide variations in hydration and Al concentration, the T_{2H} values are all ~ 1.3 ms, within a factor of about 1.4. This suggests that the Al in silica/aluminas may not be uniformly distributed throughout the silica matrix in low concentration materials. Clearly, a qualitative analysis of T_{2H} is a difficult problem, but the results we have presented so far clearly show great promise for using T_{2H} as a "spectral editing" parameter.

ZSM-5 spectral editing

This T_{2H} invariance in silica/alumina and ZSM-5, from whatever cause, makes it possible to edit ^{27}Al spectra of mixtures of ZSM-5 and silica/alumina. Such editing could be done by acquiring a single spectrum at a long τ value, where far more signal from the silica/alumina will have decayed than from the ZSM-5, but is better performed by obtaining a complete τ vs. an intensity data set, and then fitting the results to a double exponential function. *Figure 3* shows results on a mixture of γ-alumina and ZSM-5. γ-Alumina is about as difficult to edit as the silica/aluminas shown in *Table 2*, because its much higher aluminum content offsets its considerably shorter T_{2H}. Quantitative analysis on the double exponential fit generally gives good agreement (±20–40%) for both zeolitic and matrix Al contents on known mixtures, and typical 65:35 matrix/ZSM-5 materials with as little as 300 ppm zeolitic Al can be routinely quantitated. Such striking spectral editing of ZSM-5 zeolitic aluminum has not been achieved heretofore in any other n.m.r. experiment, even though the basic experiment is over 30 years old.

Zeolite-Y and spectral editing

Measuring framework (FW) aluminum in dealuminated zeolite Y should be similar to measuring FW zeolitic aluminum in a ZSM-5 γ-alumina mixture since there will be both relatively short and long T_{2H} components. An as-synthesized zeolite Y and a series of commercially available dealuminated zeolite Y samples were thus examined under static conditions, using spin-echo editing. As with the ZSM-5/γ-Al_2O_3, the decay curves appeared biexponential and were thus fit with a double exponential decay for purposes of quantitative analysis. *Figures 4* and *5* show typical echo-decay plots and a (biexponential) decay curve,

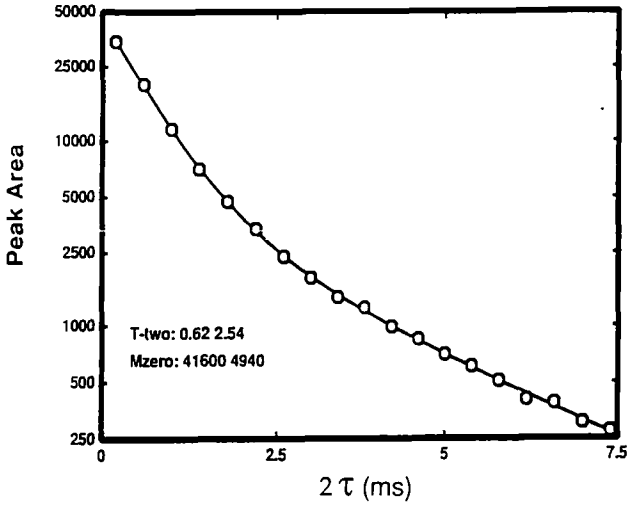

Figure 5 Typical biexponential decay for 8.45 Tesla ^{27}Al spin-echo n.m.r. data for TOSOH dealuminated Y zeolites.

Table 4 Static spin-echo ^{27}Al n.m.r. data for zeolite Y at 8.45 T

	Framework Al				Nonframework Al					
Sample[a]	% Al[b]	T_{2H} (ms)	Shift (ppm)	Width (Hz)	%Al	T_{2H} (ms)	Shift[c] (ppm)	Width (Hz)	tot Al[d] (%)	ele Al[e] (%)
NG-490	12.4	0.94	57.2	2170	–	–	–	–	12.4	9.8
HSZ-320NAA	12.3	0.82	57.7	2050	–	–	–	–	12.3	9.2
HSZ-330HSA	5.02	1.02	–	–[f]	–	–	–	–[f]	5.0	6.68
HSZ-320HOA	2.25	1.73	55.7	2190	5.17	1.02	41.5	9,270	7.4	9.3
HSZ-330HUA	0.79	2.54	56.5	2180	6.68	0.62	37.7	9,070	7.5	11.2
HSZ-360HUA	0.25	3.36	56.5	1830	4.26	0.69	33.9	10,000	4.5	5.11
HSZ-390HUA	0.0070	5.69	54.0	1810	0.058	3.10	26.5	7,950	0.065	< 0.1

[a] See Experimental section for sample descriptions
[b] Al content from n.m.r.
[c] Center of gravity of peak
[d] Total Al content, from n.m.r.
[e] Total Al content, from elemental analysis on an as-is basis
[f] No editing of FW from NFW occurs in this sample. It is presumed that this is because T_2's of the FW and NFW species are similar (~ 1 ms)

respectively. *Table 4* summarizes the T_{2H} and (absolute) Al concentration results for zeolite Y catalysts. Editing leads to a relatively constant chemical shift of 56.3 ppm and a width of 2040 Hz (27.8 ppm) for the peak assigned to FW aluminum. This shift agrees well with the 61.3 ppm derived by Lippmaa et al. for an "infinite n.m.r. field" under *MAS* conditions.[42] The width is greater than ZSM-5 (~ 10.7 ppm), reflecting the larger quadrupole coupling constant for zeolite Y than ZSM-5. However, in sharp contrast, the width and position of the NFW aluminum peak is not constant. Its chemical shift moves considerably upfield with increasing Si/Al_2, reflecting the change in tetrahedral to octahedral Al content.

There is general agreement between the total Al concentration in the zeolite obtained by using the spin-echo method and that reported by elemental analysis, given that the spin-echo technique involves fitting data to a double exponential. Much more important, however, are the results for FW aluminum. Determination of FW Al in real catalysts is generally acknowledged to be very difficult. For low Si/Al_2 samples (as-synthesized and USY), there is usually good agreement between ^{29}Si n.m.r. and spin-echo Al n.m.r. determinations, whereas for intermediate concentrations, the spin-echo technique is consistently lower than ^{29}Si n.m.r., but about the same as temperature-programmed ammonia desorption. For the highest Si/Al_2 ratio samples, the spin-echo technique is the **only** method that can be used and thus appears to have considerable potential in analyzing commercial catalyst materials.

The relationship between the second moment, M_{2F}, and T_{2H} [Equations (2) and (5)], has been discussed. For the Y zeolites in this study, M_{2F} will vary linearly with Al concentration if it is assumed that Al is distributed randomly among the zeolite lattice sites and that Lowenstein's rule is obeyed. A linear relationship between concentration and $\sqrt{M_{2F}}$ implies a linear relationship between the $1/\sqrt{[Al]}$ and T_{2H}, and as shown in *Figure 6*, we find that such a relationship does hold for the materials that we have investigated.

The T_{2H} data for the nonframework (NFW) Al support the idea that there is distorted NFW Al in zeolite Y. Four of the five dealuminated samples have very short T_{2H}s for the NFW Al, consistent with the presence of species with short Al–Al distances. At the very least, this indicates that the NFW Al does not experience the same degree of Al–Al isolation as does normal FW Al. Sample HSZ-390HUA, the highest Si/Al_2 sample, has an unusually long (3.1 ms) T_{2H} for the NFW Al, but in this case, 500 MHz ^{27}Al *MAS* n.m.r. shows that nearly all the (NFW) Al is octahedral, rather than distorted tetrahedral (FW) Al.

MAS n.m.r. experiments

All the T_{2H} results reported above were obtained on static samples. For purposes of editing broad from narrow signals, this is often the preferred approach. Conditions may exist, however, under which it is

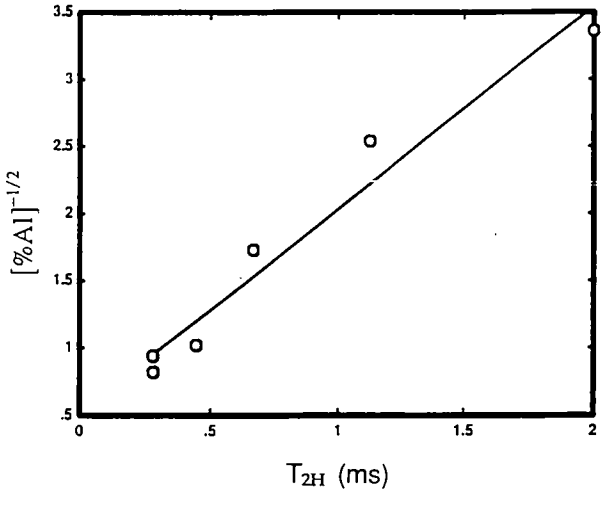

Figure 6 Plot of $1/\sqrt{[\%Al]}$ vs. T_{2H} for zeolite Y in various stages of dealumination.

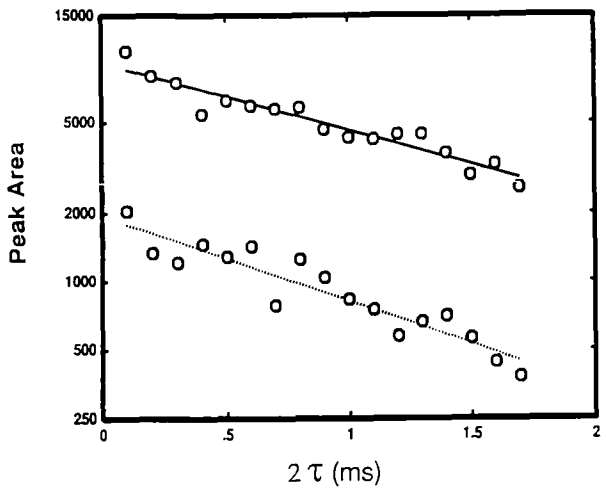

Figure 7 Plots of 2τ vs. peak area for the tetrahedral (solid line) and octahedral (dotted line) components of G-958 silica-alumina for spin-echoes obtained under *MAS* n.m.r. conditions; spinning rate = 6.000 kHz; sampling rate = 24.000 kHz.

Table 5 ^{27}Al *MAS* n.m.r. T_{2H} results

Sample	T_{2H} (ms)	Spinning rate (kHz)	Sampling rate (kHz)
NH_4–ZSM–5[a]	3.17	0.000	80.000
NH_4–ZSM–5[a]	4.53	2.000	2.000
NH_4–ZSM–5[a]	4.45	3.000	3.000
NH_4–ZSM–5[a]	4.67	4.500	4.500
NH_4–ZSM–5[a]	4.98	6.000	6.000
NH_4–ZSM–5[a]	4.94	6.024	6.024
NH_4–ZSM–5[a]	5.05	6.000	24.000
NH_4–ZSM–5[b]	5.03	0.000	80.000
NH_4–ZSM–5[b]	7.94	4.500	4.500
G-958 silica/alumina[c]	1.08	0.000	80.000
G-958 silica/alumina[c]	2.87[d]	6.000	24.000
G-958 silica/alumina[c]	1.72[e]	6.000	24.000
Corundum	0.20	0.000	80.000
Corundum	0.368	6.000	24.000
Corundum	0.432	6.000	24.000

[a] Atmospheric humidity
[b] Water-saturated
[c] Equilibrated at 52% relative humidity
[d] Tetrahedral peak
[e] Octahedral peak

desirable to take advantage of the line narrowing afforded by *MAS*, which then leads to the question of the effect of spinning of T_{2H} measurements using the spin-echo method, where moments can be expected to decrease by about the same factor (of 3–4) that quadrupole-broadened powder patterns narrow under *MAS*.[100,101] An increase in T_{2H} of $\sqrt{3}$–4, or 1.7–2 is expected and has been verified experimentally.

MAS n.m.r. experiments were carried out under conditions of synchronous sampling, i.e., the sampling of the echo signal was timed so that the rotor was always in the same position when the sampling took place. This was done so that the time-dependent part of the *MAS* Hamiltonian would be invariant for each sampling.[102] Synchronous sampling is most easily accomplished by sampling at the rotor frequency, although integer multiples give equivalent results and may be advantageous when spectra are broader (in Hz) than the spinning frequency. *Figure 7* shows spin-echo relaxation data for the tetrahedral and octahedral Al in G-958, a commercial silica/alumina. Even though the components of G-958 could be observed separately under *MAS*, it was necessary to obtain two sets of relaxation data, each with a peak on resonance, to obtain intensity vs. τ plots free of intensity oscillations.[77]

Table 5 summarizes the results. At atmospheric humidity, ZSM-5 was studied at spinning rates from 2 to 6 kHz. There is a slight, but real, increase in T_{2H} as the spinning speed increases over this range. For the four samples studied, the T_{2H}s increased by a factor of 1.6–2.1, in agreement with our previous estimate. It is clear that spectral editing, which depends on differences in T_{2H}s measured under static conditions, should also work under *MAS* conditions.

Zeolite Y in clay bound FCC catalysts is an example of a material where spin echo editing can be advantageously combined with *MAS* in order to achieve improved editing of framework zeolitic aluminum. Kaolinite is a common matrix component and will occur in calcined, steamed, or regenerated catalysts in its dehydrated metakaolinite form, so kaolinite was examined at various stages along its dehydration pathway. Static T_{2H}s of the kaolinite/metakaolinite samples were all biexponential, although the amounts of the long T_{2H} components in the natural minerals and high-temperature calcined samples were quite small, as shown in *Table 6*. These 0.6–1.6% components may be a hitherto undetected impurity phase. XRD showed a small amount of quartz forming in the otherwise amorphous high-temperature calcined phase.

The changes observed in the static T_{2H} experiments are consistent with Lambert's[84] recent experiments on kaolinite calcination. From about 300 to 600°C, dehydroxylation and conversion to metakaolinite occurs. This is accompanied by major changes in the ^{29}Si n.m.r., ^{27}Al n.m.r., and *FT*i.r. spectra. The ^{29}Si n.m.r. shows the appearance of peaks for Q4 Si at −98 and −107 ppm. The −107 ppm peak reaches its maximum intensity at about 500°C, roughly coinci-

Table 6 Effect of calcination temperature on T_{2H} and distribution of Al in calcined kaolinite

Calcination temperature (°C)	T_{2H} (ms)	%Al[a]	T_{2H} (ms)	%Al[a]
None	0.163	99.4	1.25	0.6
300	0.172	98.4	0.833	1.6
400	0.462	53.3	1.43	46.7
500	0.827	74.9	2.23	25.1
700	0.852	81.8	2.19	18.2
800	0.867	89.7	2.29	10.3
900	0.601	98.7	4.73	1.3
1000	0.586	98.6	3.39	1.4

[a] % of Al seen. This varies with calcination temperature[84]

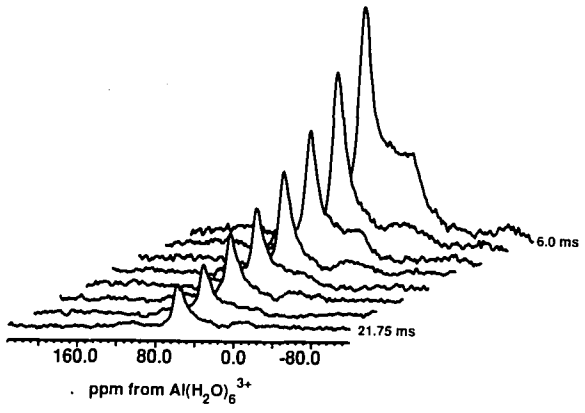

Figure 8 Synchronously sampled ^{27}Al *MAS* n.m.r. spin-echo spectra of 5 h steamed FCC catalyst at decay times (2τ) from top to bottom of 6.0, 8.25, 10.5, 12.75, 15.0, 17.25, 19.5, and 21.75 ms.

dent with the maximum in the long T_{2H} aluminum component. Pentacoordinate Al also appears and reaches a maximum over this interval. Above 900°C, metakaolinite begins to transform to mullite, and a γ-Al_2O_3-rich phase separates, according to Lemaitre et al.,[103] which is consistent with the decrease of the T_{2H} of the now 98+% component, to 0.59 ms. This agrees only qualitatively with the 0.3 ms T_{2H} measured for pure γ-Al_2O_3, but the remaining phase is not supposed to be pure γ-Al_2O_3, but, rather, γ-Al_2O_3 plus mullite (3 Al_2O_3·SiO_2) plus an Al-poor silica/alumina. It may be that the 0.59 ms T_{2H} is a composite of several similar T_{2H}'s or the phase may not be γ-alumina. The literature is not clear on the identity of this phase.[84,103–105]

More pertinent to the problem of determining FW zeolitic aluminum in clay bound FCC catalysts are the synchronously sampled *MAS* n.m.r. results for 500–700°C calcined kaolinite. *MAS* n.m.r. spin-echo editing allows separation into chemical shift regions for penta- and hexacoordinated aluminum that do not overlap the chemical shift range of zeolitic aluminum. Integration of the 70–45 ppm region, which *does* overlap the zeolitic region, shows aluminum with a (*MAS*) T_{2H} of 11.0 ms and a concentration equivalent to ~ 660 ppm Al. For the FCC catalysts, where the matrix is ~ 65% of the catalyst, this clay component will interfere with the measurement of zeolite FW Al at Si/Al_2 ~ 1000. The matrix does not interfere for the FCC catalysts of this study as shown, e.g., in *Figure 8*, where we present results for a 5 h steamed FCC catalyst. The editing leaves only the narrow peak at 60 ppm; this is typical of all the spectra and represents solely zeolitic FW Al.

Table 7 collects the FW Al concentrations, the n.m.r. chemical shifts, and the line widths determined from the *MAS* n.m.r. spin-echo experiments and the catalytic activity as measured by α. The accuracy of the FW Al results could possibly be improved slightly be deconvolution rather than by simple integration. Comparing the chemical shifts and line widths found for the edited zeolite Y in *Table 7* to the values for an as-synthesized zeolite Y indicates that the shifts are identical, within experimental error. The line widths are considerably more variable and tend to increase with the severity of treatment. The line width increases are probably not due to quadrupole broadening, since there are no accompanying upfield shifts. As observed for dealuminated Y samples of varying FW Al content, T_{2H} increases as FW Al decreases.

Most of the catalytic activity is lost during the initial calcination and essentially all the rest during the first 5 h of steaming. The remaining α changes from 1.4 to 0.8 to 0.4 or 0.6 α, are close to the experimental error limits. FW Al by *MAS* n.m.r., on the other hand, shows a much less precipitous (and monotonic) decrease, as expected[35,106] from earlier steaming studies of, e.g., ZSM-5. The loss in activity, therefore, arises from factors other than loss of FW aluminium.

CONCLUSIONS

We have reported the revival of a 30+ year old spin-echo n.m.r. technique and its application to the difficult problem of quantitatively determining small amounts of zeolitic aluminum in the presence of very large amounts of nonzeolitic aluminum. A substantial database of T_{2H} values for model Al-containing compounds is reported. We show that Al–Al dipolar interactions can predict T_{2H} reasonably well for high Al level compounds, but for compounds with low Al levels, structure-specific interactions are important, and these may be exploited for spectral editing purposes. Quantitative applications to alumina and silica/alumina bound ZSM-5 and dealuminated zeolite Y are illustrated. It is concluded that the spin-echo experiment is consistent with an NFW explanation for the "pentacoordinate" Al in zeolite Y. Theory and results for the technically somewhat more demanding measurement of T_{2H} under conditions of "magic-angle" sample spinning, with synchronous rotor sampling, are also given. Spin-echo editing of synchronously sampled ^{27}Al *MAS* n.m.r. spectra is shown to be useful for determining the framework (zeolitic) Al content of realistically formulated and steamed/calcined FCC catalysts. The loss of framework Al in

Table 7 ^{27}Al n.m.r. and catalytic data for FCC catalysts at 8.45 T

Sample	FW Al	α	T_{2H} (ms)	δ (ppm)	$\Delta\nu_{1/2}$[a] (Hz)
As-synthesized Y	–	–	–	59.8	880
Fresh REY catalyst	100[b]	25.0	4.08	58.5	1140
Calcined	41	8.1	6.62	59.8	1110
5 h steam	23	1.4	7.64	59.4	1440
10 h steam	24	0.8	7.30	60.8	800
20 h steam	19	0.4	7.42	60.2	1420
Regenerated	16	0.6	8.56	59.1	2700
USY catalyst	50	26.0	5.56	60.2	930
USY catalyst/steam	19	0.7	7.18	60.5	1130

[a] Half-height line width
[b] Corresponds to ~ 4.6% FW Al on a pure zeolite basis, or a Si/Al_2 = 18

two series of steamed FCC catalysts is less precipitous than is the loss in catalytic activity as measured by α.

ACKNOWLEDGEMENTS

This work was supported by the U.S. National Science Foundation (grants DMR 88–14789 and 89–20538) and by the Mobil Research and Development Corporation. J.H. was supported in part by the Deutsche Forschungsgemeinschaft.

REFERENCES

1 Stepanov, V.G., Shubin, A.A., Ione, K.G., Mastikhin, V.M. and Zamaraev, K.I. *Kinet. Katal.* 1984, **25**, 1225
2 Anderson, M.W., Klinowski, J. and Liu, X. *J. Chem. Soc., Chem. Commun.* 1984, 1596
3 Chang, C.D., Chu, C.T-W., Miale, J.N., Bridger, R.F. and Calvert, R.B. *J. Am. Chem. Soc.* 1984, **106**, 8143
4 Engelhardt, G., Fahlke, B., Mägi, M. and Lippmaa, E. *Z. Phys. Chem. (Leipzig)* 1985, **266**, 239
5 Scholle, K.F.M.G.J., Veeman, W.S., Frenken, P. and van der Velden, G.P.M. *J. Phys. Chem.* 1984, **88**, 3395
6 Kentgens, A.P.M., Scholle, K.F.M.G.J. and Veeman, W.S. *J. Phys. Chem.* 1983, **87**, 4357
7 Nagy, J.B., Gabelica, Z., Debras, G., Derouane, E.G., Gilson, J.-P. and Jacobs, P.A. *Zeolites* 1984, **4**, 133
8 Fyfe, C.A., Gobbi, G.C. and Kennedy, G.J. *J. Phys. Chem.* 1984, **88**, 3248
9 Fyfe, C.A., Gobbi, G.C., Klinowski, J., Thomas, J.M. and Ramdas, S. *Nature* 1982, **296**, 530
10 Derouane, E.G., Baltusis, L., Dessau, R.M. and Schmitt, K.D. *Stud. Surf. Sci. Catal.* 1985, **20**, 135
11 Smith, J.V. and Blackwell, C.S. *Nature* 1983, **303**, 223
12 Thomas, J.M., Klinowski, J. and Anderson, M.W. *Chem. Lett.* 1983, 1555
13 Ione, K.G., Vostrikova, L.A. and Mastikhin, V.M. *J. Mol. Catal.* 1985, **31**, 355
14 Geurts, F.M.M., Kentgens, A.P.M. and Veeman, W.S. *Chem. Phys. Lett.* 1985, **120**, 206
15 Gabelica, Z., Nagy, J.B., Debras, G. and Derouane, E.G. *Acta Chim. Acad. Sci. Hung.* 1985, **119**, 275
16 Debras, G., Gourgue, A., Nagy, J.B. and de Clippeleir, G. *Zeolites* 1986, **6**, 161
17 Bodart, P., Nagy, J.B., Gabelica, Z. and Derouane, E.G. *Appl. Catal.* 1986, **24**, 315
18 Gilson, J.-P., Edwards, G.C., Peters, A.W., Rajagopalan, K., Wormsbecher, R.F., Roberie, T.G. and Shatlock, M.P. *J. Chem. Soc., Chem. Commun.* 1987, 91
19 Scholle, K.F.M.G.J. and Veeman, W.S. *J. Phys. Chem.* 1985, **89**, 1850
20 Engelhardt, G., Lohse, U., Mägi, M. and Lippmaa, E., in *Structure and Reactivity of Modified Zeolites* (Eds. P.A. Jacobs et al.) Elsevier, Amsterdam, 1984, p. 23
21 Haag, W.O., Lago, R.M. and Weisz, P.B. *Nature* 1984, **309**, 589
22 Chang, C.D., Hellring, S.D., Miale, J.N., Schmitt, K.D., Brigandi, P.W. and Wu, E.L. *J. Chem. Soc., Faraday Trans. I* 1985, **81**, 2215
23 Samoson, A., Lippmaa, E., Engelhardt, G., Lohse, U. and Jerschkewitz, H.-G. *Chem. Phys. Lett.* 1987, **134**, 589
24 Hunger, M., Freude, D., Fröhlich, T., Pfeifer, H. and Schwieger, W. *Zeolites* 1987, **7**, 108
25 Freude, D., Hunger, M. and Pfeifer, H. *Z. Phys. Chem.* 1987, **152**, 429
26 Kessler, H., Chezeau, J.M., Guth, J.L., Strub, H. and Coudurier, G. *Zeolites* 1987, **7**, 360
27 Hamdan, H. and Klinowski, J. *Chem. Phys. Lett.* 1987, **139**, 576
28 Freude, D., Brunner, E., Pfeifer, H., Prager, D., Jerschkewitz, H.-G., Lohse, U. and Oehlmann, G. *Chem. Phys. Lett.* 1987, **139**, 325
29 Suzuki, K., Sano, T., Shoji, H., Murakami, T., Ikai, S., Shin, S., Hagiwara, H. and Takaya, H. *Chem. Lett.* 1987, 1507
30 Romotowski, T., Komorek, J., Mastikhin, V.M. and Nosov, A.V. *Zeolites* 1991, **11**, 491
31 Brunner, E., Ernst, H., Freude, D., Fröhlich, T. and Hunger, M. *J. Catal.* 1991, **127**, 34
32 Unger, B., Reschetilowski, W., Wendland, K.-P. and Freude, D. *Z. Chem.* 1988, **28**, 194
33 Meinhold, R.H. and Bibby, D.M. *Zeolites* 1990, **10**, 74
34 Reschetilowski, W., Einicke, W.-D., Jusek, M., Schöllner, R., Freude, D. and Klinowski, J. *Appl. Catal.* 1989, **56**, L15
35 Sano, T., Suzuki, K., Shoji, H., Ikai, S., Okabe, K., Murakami, T., Shin, S., Hagiwara, H. and Tayaka, H. *Chem. Lett.* 1987, 1421
36 Klinowski, J., Thomas, J.M., Fyfe, C.A., Gobbi, G.C. and Hartman, J.S. *Inorg. Chem.* 1983, **22**, 63
37 Klinowski, J., Thomas, J.M., Fyfe, C.A. and Gobbi, G.C. *Nature* 1982, **296**, 533
38 Freude, D., Fröhlich, T., Pfeifer, H. and Scheler, G. *Zeolites* 1983, **3**, 171
39 Freude, D. and Behrens, H.-J. *Cryst. Res. Tech.* 1981, **16**, 1236
40 Anufriev, D.M., Mastikhin, V.M., Ione, K.G. and Lapina, O.B. *Dokl. Akad. Nauk SSSR* 1978, **243**, 945
41 Grobet, P.J., Jacobs, P.A. and Beyer, H.K. *Zeolites* 1986, **6**, 47
42 Lippmaa, E., Samoson, A. and Mägi, M. *J. Am. Chem. Soc.* 1986, **108**, 1730
43 Freude, D., Fröhlich, T., Hunger, M., Pfeifer H. and Scheler, G. *Chem. Phys. Lett.* 1983, **98**, 263
44 Fyfe, C.A., Gobbi, G.C., Hartman, J.S., Lenkinski, R.E., O'Brien, J.H., Beange, E.R. and Smith, M.A.R. *J. Magn. Reson.* 1982, **47**, 168
45 Bosacek, V. and Mastikhin, V.M. *J. Phys. Chem.* 1987, **91**, 260
46 Klinowski, J., Fyfe, C.A. and Gobbi, G.C. *J. Chem. Soc., Faraday Trans. I* 1985, **81**, 3003
47 Grobet, P.J. and Jacobs, P.A. in *Proceedings of the 22nd Congress AMPERE, Zürich, 1984*, p. 379
48 Freude, D., Hunger, M. and Pfeifer, H. *Z. Phys. Chem. (Neue Folge)* 1987, **152**, 171
49 Man, P.P., Klinowski, J., Trokiner, A., Zanni, H. and Papon, P. *Chem. Phys. Lett.* 1988, **151**, 143
50 Man, P.P. and Klinowski, J. *Chem. Phys. Lett.* 1988, **147**, 581
51 Iyer, P.S., Scherzer, J. and Mester, Z.C. *Perspectives in Molecular Sieve Science*, ACS Symp. Ser. 368, Am. Chem. Soc., Washington, DC, 1988, p. 48
52 Sanz, J., Fornes, V. and Corma, A. *J. Chem. Soc., Faraday Trans. I* 1988, **84**, 3113
53 Bosacek, V. and Freude, D. in *Innovation in Zeolite Materials Science, Studies in Surface Science and Catalysis*, Vol. 37 (Eds. P.J. Grobet et al.) Elsevier, Amsterdam, 1988, p. 231
54 Hayashi, S., Hayamizu, K. and Yamamoto, O. *Bull. Chem. Soc. Jpn.* 1987, **60**, 105
55 Ray, G.J., Meyers, B.L. and Marshall, C.L. *Zeolites* 1987, **7**, 307
56 Liu, S.-B., Wu, J.-F., Ma, L.-J., Tsai, T.-C. and Wang, I. *J. Catal.* 1991, **132**, 432
57 Grobet, P.J., Geerts, H., Martens, J.A. and Jacobs, P.A. *J. Chem. Soc., Chem. Commun.* 1987, 1688
58 Fernandez, C., Lefebvre, F., Nagy, J.B. and Derouane, E.G. *Innovation in Zeolite Materials Science, Studies in Surface Science and Catalysis*, (Eds. P.J. Grobet et al.) Elsevier, Amsterdam, 1987, p. 223
59 Man, P.P. and Klinowski, J. *J. Chem. Soc., Chem. Commun.* 1988, 1291
60 Kellberg, L., Linsten, M. and Jakobsen, H.J. *Chem. Phys. Lett.* 1991, **182**, 120
61 Yue, S. and Gu, M. *Shiyou Huagong* 1991, **20**, 21
62 Flanagan, L., Report, IS-T-1518, Order No. DE91000666, 67 pp., available NTIS From Energy Res. Abstr. 1990, 15, Abstr. No. 53304
63 Nakata, S., Asaoka, S. and Segawa, K. *Nippon Kagaku Kaishi* 1989, 795

64 Jeanjean, J., Aouali, L., Delafosse, D. and Dereigne, A. *J. Chem. Soc, Faraday Trans. I* 1989, **85**, 2771
65 Haase, J., Park, K.D., Guo, K., Timken, H.K.C. and Oldfield, E. *J. Phys. Chem.* 1991, **95**, 6996
66 Fyfe, C.A., O'Brien, J.H. and Strobl, H. *Nature* 1987, **326**, 281
67 Oldfield, E., Haase, J., Schmitt, K.D. and Schramm, S.E., *Zeolites* 1994, **14**, 101
68 Beaumont, R. and Barthomeuf, D. *C. R. Acad. Sci., Ser. C* 1971, **272**, 363
69 Wu, Y., Chmelka, B.F., Pines, A., Davis, M.E., Grobet, P.J. and Jacobs, P.A. *Nature* 1990, **346**, 550
70 Mueller, K.T., Wu, Y., Chmelka, B.F., Stebbins, J. and Pines, A. *J. Am. Chem. Soc.* 1991, **113**, 32
71 Spokas, J.J. and Slichter, C.P. *Phys. Rev.* 1959, **113**, 1462
72 Alekseevski, N.E., Dautov, R.A., Krasnoperov, E.P. and Saikin, K.S. *Zh. Eksp. Teor. Fix.* 1974, **66**, 313
73 Fradin, F.Y., Brodsky, M. and Arko, A.J. *J. Phys. (Paris)* 1971, **32** (Suppl), 905
74 Greenbaum, S.G., Strom, U. and Rubinstein, M. *Phys. Rev. B* 1982, **26**, 5226
75 Resing, H.A. and Rubinstein, M. *J. Colloid Interface Sci.* 1978, **64**, 48
76 Haase, J. and Oldfield, E. *J. Magn. Res.* 1993, Series A 101, 30
77 Haase, J. and Oldfield, E. *J. Magn. Res.* 1993, Series A 104, 1
78 Lok, B.M., Messina, C.A., Patton, R.L., Gajek, R.T., Cannan, T.R. and Flannigen, E.M. US Pat. 4 440 871 (1984)
79 Breck, D.W., in *Zeolite Molecular Sieves*, Wiley, New York, 1974, p. 277
80 Delprato, F., Delmotte, L., Guth, J.L. and Huve, L. *Zeolites* 1990, **10**, 546
81 Wadlinger, R.L., Kerr, G.T. and Rosinkski, E.J. US Pat. 3 308 069 (1975)
82 Argauer, R.J. and Landolt, G.R. US Pat. 3 702 886 (1975)
83 Klotz, M.R. US Pat. 4 269 812 (1981)
84 Lambert, J.F., Millman, W.S. and Fripiat, J.J. *J. Am. Chem. Soc.* 1989, **111**, 3517
85 Johnson, C.K., A FORTRAN Thermal-Ellipsoid Plot Program for Crystal Structure Illustrations, ORNL-3794, June, 1965
86 de Saldarriaga, L.S., Saldarriaga, C. and Davis, M.E. *J. Am. Chem. Soc.* 1987, **109**, 2686
87 Batchelder, D.N. and Simmons, R.O. *J. Appl. Phys.* 1965, **36**, 2864
88 Newnham, R.E. and de Haan, Y.M. *Z. Kristallogr.* 1962, **117**, 235
89 Schulz, H. and Thieman, K.H. *Solid State Commun.* 1977, **23**, 815
90 Ng, H.N. and Calvo, C. *Can. J. Phys.* 1976, **54**, 638
91 Olson, D.H. *J. Phys. Chem.* 1970, **74**, 2758
92 Pluth, J.J. and Smith, J.V. *J. Am. Chem. Soc.* 1980, **102**, 4704
93 Higgins, J.B., personal communication
94 Qui, S., Pang, W., Kessler, H. and Guth, J.-L. *Zeolites* 1989, **9**, 440
95 Pluth, J.J., Smith, J.V. and Bennett, J.M. *Acta Crystallogr.* 1986, **C42**, 283
96 Richardson, J.W., Jr., Pluth, J.J. and Smith, J.V. *Acta Crystallogr.* 1988, **B44**, 373
97 Higgins, J.B., LaPierre, R.B., Schlenker, J.L., Rohrman, A.C., Wood, J.D., Kerr, G.T. and Rohrbaugh, W.J. *Zeolites* 1988, **8**, 446
98 Olson, D.H., Kokotailo, G.T., Lawton, S.L. and Meier, W.M. *J. Phys. Chem.* 1981, **85**, 2238
99 Boulogne, B., Cordier, P., Doukhan, B. and Boulogne, J.-C. *Phys. Chem. Minerals* 1988, **16**, 250
100 Abragam, A., in *Principles of Magnetic Resonance*, Oxford University Press, London, 1961, p. 131
101 Ganapathy, S., Schramm, S. and Oldfield, E. *J. Chem. Phys.* 1982, **77**, 4360
102 Yarim-Agaev, Y., Tutunjian, P.N. and Waugh, J.S. *J. Magn. Reson.* 1982, **47**, 51
103 Lemaitre, J., Leonard, A.J. and Delmon, B., in *Proceedings of the International Clay Conference, 1975* (Ed. S.W. Bailey) Applied Publishing, 1976, p. 544
104 Sanz, J., Madani, A., Serratosa, J.M., Moya, J.S. and Aza, S. *J. Am. Ceram. Soc.* 1988, **71**, 418
105 Rocha, J. and Klinowski, J. *Phys. Chem. Miner.* 1990, **17**, 179
106 Lago, R.M., Haag, W.O., Mikovsky, R.J., Olson, D.H., Hellring, S.D., Schmitt, K.D. and Kerr, G.T. *Stud. Surf. Sci. Catal.* 1986, **28**, 677